Astronomy & Astrophysics manuscript no.
(will be inserted by hand later)

Intense accretion and mass loss of a very low mass young stellar object ⋆

M. Fernández[1] and F. Comerón[2]

[1] Instituto de Astrofísica de Andalucía, CSIC, Apdo. 3004, E-18080 Granada, Spain (matilde@iaa.es)
[2] European Southern Observatory, Karl-Schwarzschild-Strasse 2, 85748 Garching, Germany (fcomeron@eso.org)

Received; accepted

Abstract. We present visible and near-infrared photometry and spectroscopy of LS-RCrA 1, a faint, very late-type object (M6.5-M7) seen in the direction of the R Coronae Australis star forming complex. While its emission spectrum shows prominent features of accretion and mass loss typical of young stellar objects, its underlying continuum and photometric properties are puzzling when trying to derive a mass and age based on pre-main sequence evolutionary tracks: the object appears to be far too faint for a young member of the R Coronae Australis complex of its spectral type. We speculate that this may be due to either its evolution along pre-main sequence tracks being substantially altered by the intense accretion, or to a combination of partial blocking and scattering of the light of the object by a nearly edge-on circumstellar disk. The rich emission line spectrum superimposed on the stellar continuum is well explained by an intense accretion process: the H_α, CaII infrared triplet, and HeI 6678 lines show equivalent widths typical of very active classical T Tauri stars. The near-infrared observations show anomalously weak spectral features and no significant excess emission in the K band, which we tentatively interpret as indicating line filling due to emission in a magnetic accretion funnel flow. At the same time, numerous, strong forbidden optical lines ([OI], [NII] and [SII]) and H_2 emission at 2.12 μm suggest that the object is simultaneously undergoing mass loss, providing another example that shows that mass loss and accretion are closely related processes. Such an intense accretion and mass loss activity is observed for the first time in a young stellar object in the transition region between low mass stars and brown dwarfs, and provides a valuable observational test on the effects of accretion on the evolution of objects with such low masses.

Key words. Stars: circumstellar matter; low-mass and brown dwarfs; mass-loss; pre-main sequence; winds, outflows. Open clusters and associations: R Coronae Australis.

1. Introduction

Many of the distinctive features that characterize young stellar objects are related to the mass accretion and mass loss processes that accompany the earliest stages of stellar evolution. Although such processes are present all over the stellar mass spectrum, their observational manifestation adopts a variety of forms depending on the mass of the forming object. In the case of low mass pre-main sequence stars, the optical features arising from accretion give rise to their classification as classical T Tauri stars (CTTS; Bertout 1989, Appenzeller & Mundt 1989). Due to angular momentum conservation, the matter from the envelope falls first on the so-called *accretion disk*. In the frame of the magnetospheric accretion model (see Hartmann 1998 for a comprehensive review), the matter ultimately falls onto the star moving along the magnetic field lines. A large amount of energy is involved in this process; nevertheless, the intrinsic stellar luminosity dominates over the accretion emission for spectral types earlier than $\sim$ K5, and the features that provide us with most of the information have to compete with a strong continuum. Attempts to circumvent this difficulty include: a) observations at ultraviolet wavelengths, where the stellar continuum drops significantly (e.g. Gullbring et al. 2000) and the emission is greatly enhanced due to the high temperatures reached by the gas shocked upon reaching the stellar surface (Calvet & Gullbring 1998, Gullbring et al. 1998), or b) the optical study of very low mass (i.e., intrinsically faint) stars.

The study of accretion in very low mass objects also allows us to address the issue of how this process changes with the depth of the central potential well, which is a major factor governing its dynamics. The considerable theoretical effort devoted to modeling the spectrum of accreting stars has understandably focused on young stel-

Send offprint requests to: M. Fernández

⋆ Based on observations collected at the European Southern Observatory in La Silla and Cerro Paranal (Chile), in programs 59.E-0679, 63.I-0546, 264.I-5723, 64.L-0049, 65.H-0492, and 67.C-0109.

lar objects with masses of a few tenths of a solar mass (Hartmann 1998), which is the range occupied by the vast majority of CTTS observed in detail so far. However, signposts of moderate mass accretion have been detected recently in very low mass stars and even young brown dwarfs (Luhman et al. 1997, Comerón et al. 2000, Muzerolle et al. 2000), whose masses are in the range of *hundredths* of a solar mass. H_α emission in very young objects with masses as low as ~ 0.01 $M_\odot$, or perhaps even less, has been very recently reported by Zapatero-Osorio et al. 2000 in the σ Orionis cluster.

A natural question is whether objects near the bottom of the main sequence or below can display the signs of strong accretion observed at higher masses, or rather the low central masses limit accretion to very low rates unable to display the rich emission spectra sometimes found in solar-type stars. In this paper we present both visible and near-infrared observations of a newly discovered, late-type object in the R Coronae Australis (R CrA) star forming region with strong emission at H_α and other lines, including forbidden lines typically associated with mass loss. The late spectral type combined with the young age implied by its membership in the star forming region place this object near the borderline between very low mass stars and brown dwarfs, demonstrating that signposts of intense accretion and mass loss can indeed be found even at such low masses. However, we find very serious difficulties in reconciling the observed spectral and photometric properties of this object with the predictions of pre-main sequence evolutionary models. We tentatively interpret this as a sign of an early evolutionary story dramatically modified by accretion, or as the result of combined extinction and scattering by a circumstellar disk seen almost edge-on.

Our observational material is presented in Section 2, and our results concerning the intrinsic properties of the object, as well as its accretion and mass loss signposts, are described in Section 3. The results are discussed in Section 4, and conclusions are summarized in Section 5.

2. Observations

The initial observations leading to the identification of the object discussed in this paper (hereafter referred to as LS-RCrA 1, where LS stands for La Silla following the tradition inaugurated by the IAC group of naming very low mass objects after the observatory from where they were discovered) consisted of slitless spectroscopy of the central region of the R CrA complex, carried out with the 1.5 Danish telescope in La Silla in April 1999. Short imaging in the BVR_C filters was obtained followed by deeper slitless spectroscopic integrations in which a Gunn r filter was used to isolate the H_α region and reduce the bright background caused by moonlight. For extraction of the spectra, the R_C-band image of the field was used to link a reference star with its spectrum in the slitless spectroscopy frame, manually defining the spectrum extraction area. In this way, the position of the spectrum relative to the image of the object was determined. Next, sources were automatically detected in the image frame using DAOPHOT, and a spectrum was extracted for each one using the offset between the image of the star and its spectrum as defined from the reference star. A review of all the spectra obtained in this way allowed an easy and fast selection of late-type H_α-emitting targets as judged from the appearance of the stellar continuum feature at 6800 Å $< \lambda <$ 7100 Å.

In these observations, LS-RCrA 1 stands out due to a clearly visible H_α emission on an undetected continuum. Other previously-known late H_α-emitting objects (Marraco & Rydgren 1981, Graham 1993) were detected too, as well as another, brighter late M dwarf with very weak H_α emission, hereafter called LS-RCrA 2. The measured magnitudes of LS-RCrA 1 ($B = 22.6$, $V = 20.9$, $R_C = 19.5$) at the time of those observations made it the faintest H_α-emitting object identified so far in R CrA, perhaps indicating a mass below the hydrogen-burning limit.

Follow-up observations in the visible were carried out in service mode on 29 March 2000 using FORS2, one of the imagers and low resolution spectrographs at the ESO Very Large Telescope (VLT). A spectrum was obtained by combining a series of 5 individual spectra taken using a slit of 1"4 of aperture and a grism yielding a dispersion of 2.6 Å pix^{-1}. The resulting spectrum covers the range 5940 Å-10000 Å at a resolution $R \simeq 500$. Relative flux calibration was performed with reference to the spectrophotometric standard EG274 (Hamuy et al. 1992). Wavelength calibration was performed by taking an exposure of a HeAr lamp using the same instrumental setup as with the science exposures.

Observations in the near-infrared were obtained with ISAAC, the infrared imager and spectrograph at the VLT, in visitor mode. By a fortunate coincidence, the service observations with FORS2 were scheduled for the same night when the ISAAC spectroscopy was performed, and therefore the observations in both spectral regions are simultaneous. The ISAAC observations cover the K band between 2.0 μm and 2.4 μm at a resolution of $R = 830$. Telluric features were removed by rationing the spectrum of LS-RCrA 1 by that of HD 188112, a B9V star near its position in the sky and observed at a very similar airmass. Wavelength calibration was performed using sky airglow lines (Oliva & Origlia 1992).

Besides the BVR_C photometry obtained at the time of the slitless spectroscopic survey, we reobserved the field of LS-RCrA 1 on 29 August 2000 using the Wide Field Imager (WFI) at the ESO-MPI 2.2m telescope in La Silla. The BVR_CI_C filters were used with the main goal of checking for possible variability. Infrared imaging of the field in the JHK bands was performed with SOFI, the near-infrared camera and spectrograph at the ESO New Technology Telescope (NTT) on 28 February 2000. Both the April 1999 and the August 2000 images were flux-calibrated using late-type stars in the same field with previously published photometry: the B and V magnitudes were calibrated using stars in common with the catalog of Marraco & Rydgren 1981. For the R_C and I_C filters

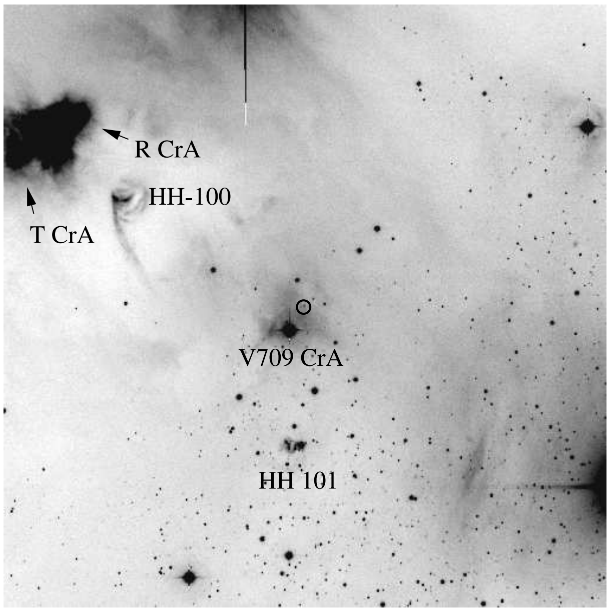

Fig. 1. R_C-band image of the region around LS-RCrA 1 obtained with the Wide Field Imager. The field shown here is centered on the object, which is the faint encircled source to the top right of V709 CrA. Its coordinates are $\alpha(2000) = 19^h01^m33\overset{s}{.}7$, $\delta(2000) = -37°00'30''$, and the field shown is $10'7 \times 10'7$ across, with North at the top and East to the left. Other members of the star forming region, both stellar and non-stellar, are indicated.

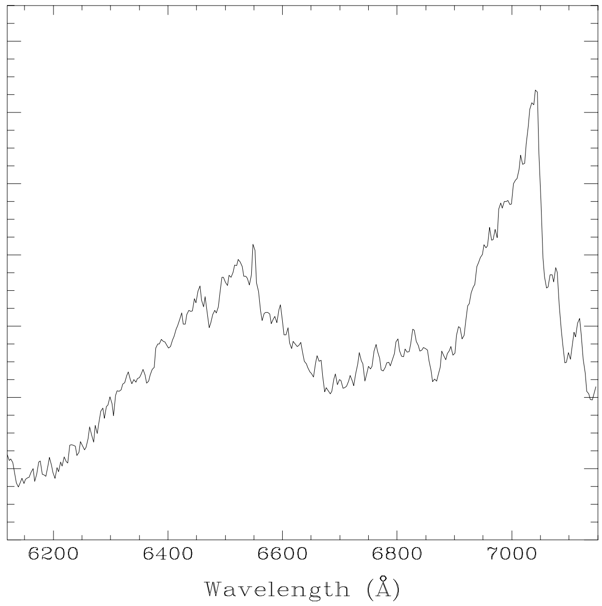

Fig. 2. Extracted slitless spectrum of LS-RCrA 2 from the DFOSC observations of April 1999. H_α emission is barely visible at 6561 Å. The vertical axis is in arbitrary flux units and has its origin at zero.

we used instead the magnitudes listed by Patten 1998, as Rydgren & Marraco's R and I magnitudes are in the Johnson system. The near-infrared photometry was calibrated using as a reference stars in the field from the survey of Wilking et al. 1997. Finally, an additional snapshot image of LS RCrA 1 was obtained with ISAAC on 30 April 2001 during excellent seeing conditions (0"38 FWHM in the K band) in order to probe any possible small extended structure around the object.

3. Results

Figure 1 shows a visible image of LS-RCrA 1 and the field surrounding it, obtained from the WFI observations. The field is centered at the position of the object, $\alpha(2000) = 19^h01^m33\overset{s}{.}7$, $\delta(2000) = -37°00'30''$. Previously identified members of the R CrA complex are indicated in the image, as well as the nebulosity associated to the Herbig-Haro objects HH 100 and HH 101. Table 1 gives the available multiband photometric measurements for LS-RCrA 1. The 1-σ errors quoted include the contribution of the uncertainty in the zero points derived from the reference stars in the field, that we take as 0.1 mag in each band. Hints of variability are inferred from the comparison between the photometric measurements of April 1999 and August 2000. These are confirmed at near-infrared wavelengths by comparing our February 2000 magnitudes to those published by Wilking et al. 1997, that are fainter by 0.2 at K and slightly bluer, by 0.1 mag in $(J-K)$, although the latter effect is not significant in view of the associated error bars.

Figure 2 shows the slitless spectrum of LS-RCrA 2, for which no follow-up observations were carried out, and Table 2 summarizes its main characteristics. Its positions on the $(J-H)$,$(H-K)$ diagram and on the temperature-luminosity diagram are shown in Figs. 5 and 7, respectively. No significant differences are found between the BVR_C photometry obtained in April 1999 and that of August 2000 within the respective uncertainties, and we list the latter in Table 2 due to its higher expected accuracy. Although we did not observe LS-RCrA 2 in the infrared, this object is included in the survey of Wilking et al. 1997 and we have used their photometry here. The procedure followed to estimate its physical properties is the same that we describe below applied to LS-RCrA 1 (See Sections 3.4 and 3.5), neglecting reddening as the measured $(J-H)$ is already near the typical value of dereddened late-type M stars (Section 3.4). The slitless spectrum of LS-RCrA 2 looks very similar to that of Cha Hα 4 obtained with identical setup (Comerón et al. 1999), that Comerón et al. 2000 classify as M6. The same spectral type is thus adopted here for LS-RCrA 2, whose features are those of a young very low mass star or massive brown dwarf without noticeable near-infrared excess.

3.1. Spectral classification in the visible

In the remainder of this paper we focus our attention on LS-RCrA 1. Its visible spectrum in the red obtained with FORS2 in March 2000, displayed in Fig. 3, shows the striking appearance of numerous strong emission lines superimposed on a late-type continuum. The vertical scale is

Table 1. Magnitude measurements of LS-RCrA 1.

Date	B	V	R_C	I_C	J	H	K
April 1999	22.6 ± 0.2	20.89 ± 0.12	19.45 ± 0.11				
February 2000					15.28 ± 0.10	14.45 ± 0.10	13.90 ± 0.10
August 2000	23.06 ± 0.13	21.34 ± 0.11	19.76 ± 0.10	18.02 ± 0.10			

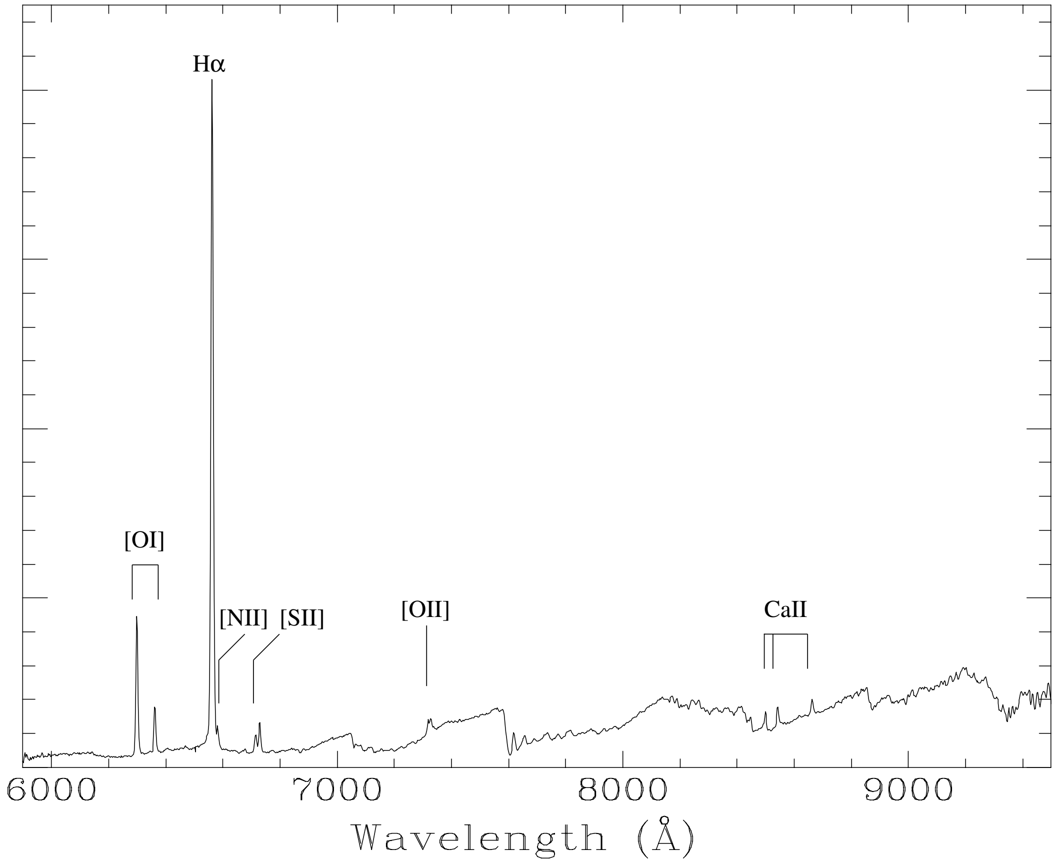

Fig. 3. Overall appearance of the red spectrum of LS-RCrA 1 obtained with FORS2. The main emission lines are identified.

enlarged in Fig. 4 in order to show in detail the continuum, with the main features identified. The photospheric spectrum shows all the characteristics expected from a late type object, being dominated by deep TiO and VO bands (Kirkpatrick et al. 1991). Among the atomic features, the lack of prominent NaI absorption at 8190 Å is an indication of the low surface gravity expected in a young cool object in its early contraction stages. A comparison to the spectral sequence of Chamaeleon I late-type objects (Comerón et al. 2000), expected in principle to have ages and intrinsic physical characteristics close to those of LS-RCrA 1, allows us to classify it as M6-M7. The spectral type determination may be somewhat affected by continuum veiling, to be expected even at such relatively long wavelengths given the intense accretion signs in the visible spectrum of this object. However, the shape of the spectral features, that should be relatively unaffected by a featureless veiling, clearly show that the spectral type cannot be as late as M8. Adopting M6.5 as the spectral type of LS-RCrA 1, as we do in the rest of the discussion unless otherwise indicated, thus seems a safe estimate.

3.2. Emission-line spectrum

The most apparent characteristics of the visible spectrum of LS-RCrA 1 are the intense emission lines superimposed on the late-type continuum; their equivalent width measurements are listed in Table 3.

The forbidden emission lines of [OI], [SII] and [NII] have been attributed in the literature to low density regions such as winds, and are therefore a tracer of the mass loss process. In particular, the intensity ratio of the [SII] 6716 line to the [SII] 6731 line gives information about the electronic density. We get a value of 0.65 that is within the range of values that Cabrit et al. 1990 and Hamann 1994 found for several CTTSs and very close to the largest values, which are found for RW Aur (0.68) and HL Tau (0.77). RW Aur powers a flow, for which Dougados et al.

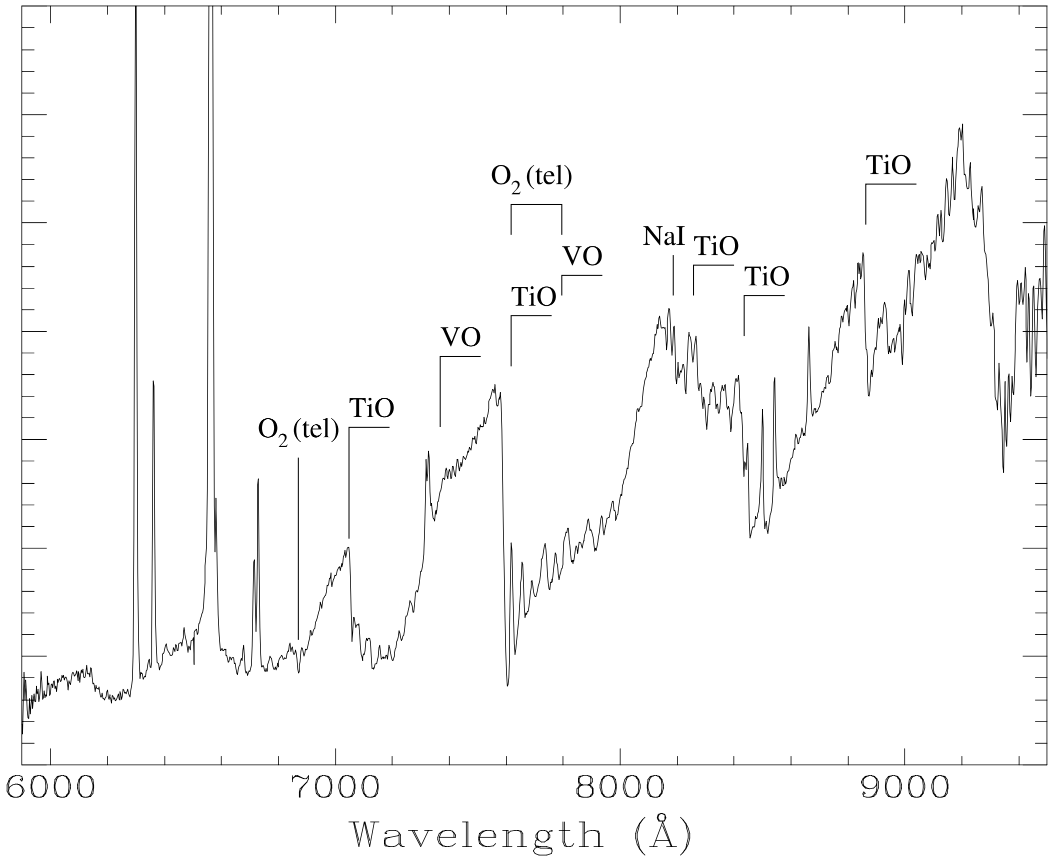

Fig. 4. An enlargement of Fig. 3 in the vertical direction, showing in detail the underlying continuum of LS-RCrA 1. The main photospheric and telluric features are marked.

Table 2. Characteristics of LS-RCrA 2

$\alpha(2000)$	$19^h01^m49\overset{s}{.}5$
$\delta(2000)$	$-37°00'28''$
B^1	19.13
V^1	17.11
R_C^1	15.84
I_C^1	14.18
J^2	12.54
H^2	11.81
K^2	11.64
Spectral type	M6
W(H_α)	1.2-2.1 Å
Temperature	2990 K
Luminosity Log($L/L_\odot$)	-1.54
Age[3]	4 Myr
Mass[3]	0.08 $M_\odot$

Notes:
[1]: Visible photometry obtained with the WFI in August 2000.
[2]: Infrared photometry from Wilking et al. 1997.
[3]: Age and mass from Baraffe et al. 1998 models.

2000 have resolved the emission very close to the star (microjet).

Table 3. Equivalent widths of the identified emission lines on the visible spectrum of LS-RCrA 1

Identification	λ_{obs}	W(line) (Å)
[OI]	6299	92
[OI]	6362	25
H_α	6562	360
[NII]	6581	15
He I	6678	1.5
[SII]	6714	12.4
[SII]	6729	19.2
[OII]	7319	3.6
[OII]	7329	3.6
CaII	8499	4.0
CaII	8543	3.6
CaII	8663	2.2

Comparing the forbidden line spectrum to those of other CTTSs, we find a strong resemblance to that of the K-type star Th-28 (HBC 617). They both show similar intensity ratios for the forbidden lines and even the small bump on the red wing of the [OI]6300, attributed to the [SIII]6312 line. Schwartz 1977 suggested that Th-28 could be a star embedded in a HH nebula. This suggestion was confirmed by Krautter (1986; see also Krautter et al. 1984), who discovered that the star was the exciting source of a bipolar HH jet. The exciting source of HH 34, a G- or K-type star that powers a 3-parsecs jet (Bally & Devine 1994) shows a similar emission-line spectrum, although with different intensity ratios (Reipurth et al. 1986).

Since the emission lines that characterize mass accretion are also common to outflows, the presence of mass loss may thus mask the signatures of the accretion process. Nevertheless, the ratio of equivalent widths between the H_α and the [SII] lines in LS-RCrA 1 is 11, far too large for the emission spectrum to be outflow-dominated. This ratio does not exceed 4 in HH objects (e.g. Böhm & Goodson 1997); for example, HH 80A, powered by a 2×10^4 $L_\odot$ source, is among those that show highest excitation, with a ratio of 3.7 (Heathcote et al. 1998). We thus conclude that, even in the most extreme case, at least 2/3 of the H_α emission in the spectrum of LS-RCrA 1 is related to accretion, rather than outflow activity.

The CaII infrared lines are also observed in both HH objects and strongly accreting stars. The equivalent widths that we have measured for the three components of this triplet are similar, while the predicted ratio for optically thin emission is 1:9:5. Ratios close to 1:1:1, like the one we find in our case, are common among CTTS undergoing strong-to-moderate mass accretion and showing no [SII]6731 emission, i.e., no signatures of outflows. Reipurth et al. 1986 found similar ratios for the exciting source of HH34, and Graham & Heyer 1988, who also found the same ratios for Th-28, conclude that saturation is occurring and that the lines are being formed close to the stellar surface. Such ratios are markedly different from those of HH flows. This supports our interpretation that the emission features common to mass accretion and mass loss are dominated by the former cause in the case of LS-RCrA 1. The HeI 6678 line is another evidence of the mass accretion process.

Nevertheless, the strength of this accretion process can be, despite the strong emission lines, not unusual in the frame of the well known CTTSs. The intensity ratio (K5 star)/(M6 star) of the continuum at the wavelength range covered by the mentioned emission lines is larger than an order of magnitude. Therefore, equivalent widths should be corrected by this factor before any comparison is done.

3.3. Near-infrared properties

Figure 5 shows the position of LS-RCrA 1 in a $(J-H)$, $(H-K)$ diagram, which is the usual diagnostic tool to reveal excess emission of circumstellar origin (e.g. Lada & Adams 1992). The plotted position is based on the February 2000 photometry, but a very similar one is obtained when using the JHK photometry of Wilking et al. 1997. For reference, very low mass young objects in other star forming regions with spectral types bracketing that of LS-RCrA 1 are plotted as well. The location of LS-RCrA 1 in the diagram does not indicate any significant amount of near-infrared excess, at least at the dates of the photometric observations.

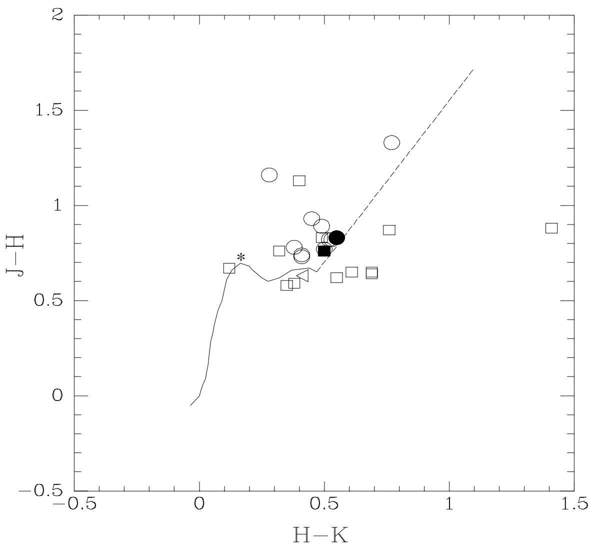

Fig. 5. $(J-H)$, $(H-K)$ diagram showing the position of LS-RCrA 1 (filled circle) and of LS-RCrA 2 (asterisk) with respect to the main sequence locus (solid line, Bessell & Brett 1988). The dashed line is the reddening vector from Rieke & Lebofsky 1985 for a visual extinction $A_V = 10$ mag, with its origin placed at the position of a M6 star. For comparison, the position of other very low mass objects in other star forming regions are plotted as well (open circles: Chamaeleon I data, Comerón et al. 2000; open squares: IC 348 data, Luhman 1999; open triangle: V410 X-ray 3, Luhman 2000; filled square, Oph162349.8-242601, Luhman et al. 1997. For the latter, the near-simultaneous photometry of Barsony et al. 1997 has been adopted).

The K band spectrum obtained with ISAAC in March 2000 is shown in Fig. 6. In principle, the visibility of the CO bandheads starting with the $v = 0 \rightarrow 2$ transition at 2.29 μm seems consistent with the late spectral type derived from observations in the visible-red. However, the equivalent widths of these bands are well below those commonly seen in late-type young objects: for the $v = 0 \rightarrow 2$ band, the 5 Å that we measure are only one third of the equivalent width normally seen at M6 (Luhman & Rieke 1998). Even more surprising is the absence of atomic features that should be readily detected at this resolution. With the possible exception of MgI, no features are seen with equivalent widths above 3 Å, while the NaI and probably CaI lines should be clearly seen.

Veiling by a continuum due to disk emission is a commonly invoked cause of the decrease in the strength of spectral features in young stellar objects (Casali & Matthews 1992, Casali & Eiroa 1996, Greene & Lada 1996a), and may be explored as a possible explanation for LS-RCrA 1 as well. Veiling is characterized by the index r_K defined as:

$$r_K = \frac{I_{2.2}(\text{excess})}{I_{2.2}(\text{intrinsic})} \tag{1}$$

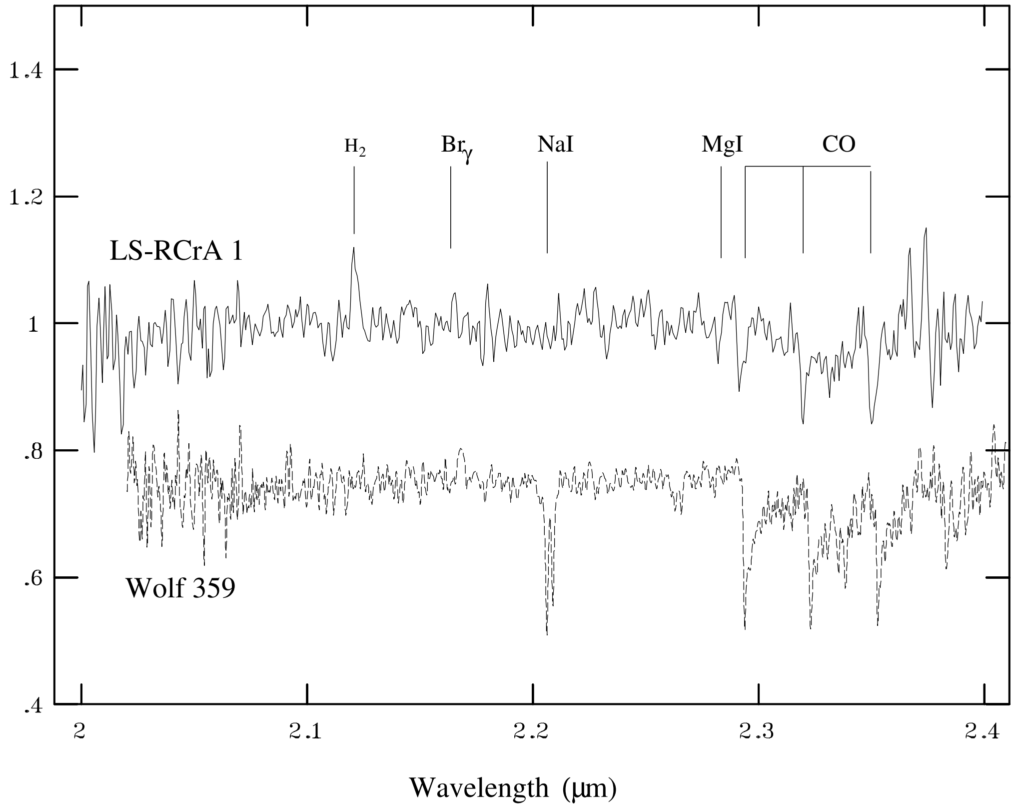

Fig. 6. K-band spectrum of LS-RCrA 1 obtained with ISAAC at the VLT. The intensity has arbitrary units and a base line of 0. The most prominent features are marked, as well as the positions of other features commonly appearing in low- to mid-resolution spectra of late-type objects and that are absent from the present one. Below: the spectrum of an M6 standard star (Wolf 359, Kleinmann & Hall 1986) is plotted with a dashed line; it has been shifted from its position at continuum equal to 1.

where "intrinsic" refers to the photospheric emission of the object if it were devoided of circumstellar emission, and "excess" is the emission above that level produced by the circumstellar material. The subindex "2.2" means that the parameter is measured at 2.2 μm. In terms of equivalent widths,

$$r_K = \frac{W_{\rm int}}{W_{\rm veiled}} - 1 \qquad (2)$$

where $W_{\rm int}$ is the equivalent width that the line would have in the absence of veiling, and $W_{\rm veiled}$ is the measured one. We can estimate r_K from the first CO bandhead ($W_{\rm veiled}$ = 5 Å), assuming that it has $W_{\rm int}$ = 15 Å (see Fig. 8 of Luhman & Rieke 1998). We thus obtain $r_K = 2$, meaning that only 1/3 of the flux at K comes from photospheric emission. However, this assumes that the veiling is featureless, neglecting the possibility that the circumstellar disk responsible for the veiling has its own CO bands in emission as is sometimes observed, even in very low luminosity objects (Greene & Lada 1996b). If the weakening of the CO bands is due to filling by disk emission, then $r_K = 2$ is an upper limit to the veiling. On the other hand, we can derive a lower limit based on the non-detection of NaI and assuming a normal $W_{\rm int} \simeq 5$ Å for this line in a M6.5 object (Luhman & Rieke 1998). The non-detection of NaI down to a limit of 3 Å together with the discussed weakening of the CO features thus yields $0.7 < r_K < 2$.

These limits imply a considerable or even dominant contribution of circustellar emission to the K-band flux, as would be expected in class I or flat-spectrum sources (Greene & Lada 1996a). However, in all those cases the same hot dust responsible for veiling causes a steeply rising overall spectral energy distribution that is in sharp contrast with the normal position of LS-RCrA 1 in the $(J-H)$, $(H-K)$ diagram. Strong variability of the near-infrared spectrum shape or the veiling cannot be a cause: relative flux calibration (Fig. 6) shows that the overall shape of the spectrum is nearly flat as corresponding to a unreddened late-type object without circumstellar emission. This strongly argues against veiling as the responsible mechanism for the nearly disappearance of spectral features in the K band.

An attractive alternative, especially in view of the unique accretion features seen at visible wavelengths, is the possibility of line filling due to line emission in accretion funnel flows (Martin 1996). Line formation near the base of the accretion column of infalling gas from the magnetically disrupted circumstellar disks can explain many features displayed by T Tauri stars. Most interestingly for the present discussion, this mechanisms predicts that the line emission, including CO band emission (Martin

1997), should take place without being accompanied by continuum excess due to dust. This may thus simultaneously explain the weakening of infrared absorption features and the normal near-infrared colors. Higher resolution observations are needed to confirm this possibility. If confirmed, detailed radiative transfer calculations may set useful constraints on the physical conditions of the accreting gas implied by our simultaneous observation of a very strong H_α line and no significant Brγ emission.

The only other feature that is apparent in the infrared spectrum of LS-RCrA 1 besides the CO bands is the emission line due to H_2 v=1-0 S(1) at 2.12 μm. H_2 emission is also frequently observed in accreting objects heavily shrouded in circumstellar material (Greene & Lada 1996a), and in this respect it may be considered as a "class I-like" feature of LS-RCrA 1. Given the usual appearance of H_2 as a tracer of molecular outflows and the relatively strong forbidden lines indicative of mass loss in the visible spectrum, it may not be surprising to find H_2 emission in the spectrum of LS-RCrA 1.

We note that H_2 emission has been observed as well in the candidate brown dwarf GY 11 in the ρ Ophiuchi embedded cluster (Williams et al. 1995; Wilking et al. 1999), an object known to possess considerable excess emission in the thermal infrared (Comerón et al. 1998). Unlike in the case of GY 11, an inspection of the original frames from which the spectrum was extracted does not show the H_2 feature in LS-RCrA 1 to be extended.

3.4. Temperature and luminosity

We now turn to the estimate of the intrinsic properties of the central object in LS-RCrA 1. Adopting the temperature vs. spectral type calibration proposed by Luhman 1999 for very young M-type objects (see also discussion in Comerón et al. 2000), the temperature corresponding to a spectral type M6.5 is $T_{\rm eff} = 2910$ K. This temperature is intermediate between those of field dwarfs and red giants of the same spectral type; taking the temperature scale of field dwarfs as a limiting case, and assuming an error in the spectral type allocation of 0.5 spectral subclasses, we can take $T_{\rm eff} = 2720$ K, corresponding to a M7 field dwarf (extrapolated from Leggett et al. 1996) as a lower limit to the temperature of LS-RCrA 1.

The observed $(J-H)$ color of LS-RCrA 1, 0.83, is near the intrinsic colors observed among young late-type objects. We choose this color to estimate the intrinsic properties as being the one less affected by the potential effects of veiling at bluer wavelengths and circumstellar disk emission further into the infrared. The dereddened $(J-H)_0$ color derived from the sample of young late-M objects in Chamaeleon I of Comerón et al. 2000 is $(J-H)_0 = 0.77 \pm 0.05$ without a noticeable variation with spectral type over the range M6-M8, and it seems to be an appropriate choice in the present case as well. This value is similar to the average of 0.72 found from the JHK photometry of Pleiades objects in the same spectral type interval by Zapatero-Osorio et al. 1997. Adopting $(J-H)_0 = 0.77$ and the near-infrared extinction law of Rieke & Lebofsky 1985, one obtains a J-band extinction of $A_J = 0.13$, which may be increased to 0.26 if the Pleiades average of $(J-H)_0 = 0.72$ is adopted instead. The relatively blue BVR_CI_C colors, being similar to those of unreddened field M6V dwarfs (Kenyon & Hartmann 1995) rule out in principle significantly higher values of the extinction; see however the discussion in Section 3.5.

We have used the bolometric correction at J (BC_J) vs. spectral type relationship of Lawson et al. 1996 to estimate the intrinsic luminosity of the LS-RCrA 1. BC_J presents the advantage over bolometric corrections at shorter wavelengths of a smaller absolute value and a smaller sensitivity to the spectral subclass (as can be seen for instance from the comparison between the relationship for dwarfs from Lawson et al. 1996 and that for giants from Fluks 1998). The value that we adopt here is $BC_J = 1.95$, for which we estimate an uncertainty of 0.2 mag from the difference between those relationships at spectral type M6.5. This may be a rather pessimistic estimate, given the much closer spectral resemblance of very young objects to dwarfs than to giants.

As for the distance to the R CrA star forming region, existing measurements cover a range of about 50 pc in width centered at $\simeq$ 150 pc. The most widely adopted value is 130 pc, from Marraco & Rydgren 1981, corresponding to a distance modulus $DM = 5.6$. De Zeeuw et al. 1999 find this to be compatible with *Hipparcos* measurements, but they note that no meaningful parallaxes could be measured by *Hipparcos* for members of the star forming region. However, based on *Hipparcos* parallaxes for obscured stars located behind the cloud, Knude & Høg 1999 propose a distance of 170 pc, corresponding to $DM = 6.15$. Other published distance determinations for the R CrA region are summarized in Neuhäuser et al. 2000. We adopt here $DM = 5.9$ as the distance modulus of LS-RCrA 1, as a compromise among all existing measurements in the quoted range.

These measurements thus suggest no significant difference between the distance to R CrA and that to other nearby low-mass star forming regions like Taurus, ρ Ophiuchi or Chamaeleon. However, comparison of the photometry given in Table 1 with the results of studies of the low-mass component in those other regions shows that LS-RCrA 1 is considerably *fainter* than other objects of similar spectral type and expected to have a similar age. Indeed, the luminosity derived from

$$\log L(\mathrm{L}_\odot) = 1.86 - 0.4(J - A_J - DM + BC_J) \qquad (3)$$

adopting our photometry and the values for A_J, DM and BC_J discussed in the previous paragraphs yield $\log L(\mathrm{L}_\odot) = -2.63$. This is only a little more than half of the luminosity of the faintest M8 brown dwarf identified by Comerón et al. 2000 in Chamaeleon I. We might assume that all the uncertainties discussed in previous paragraphs conspire to decrease our derived luminosity with respect

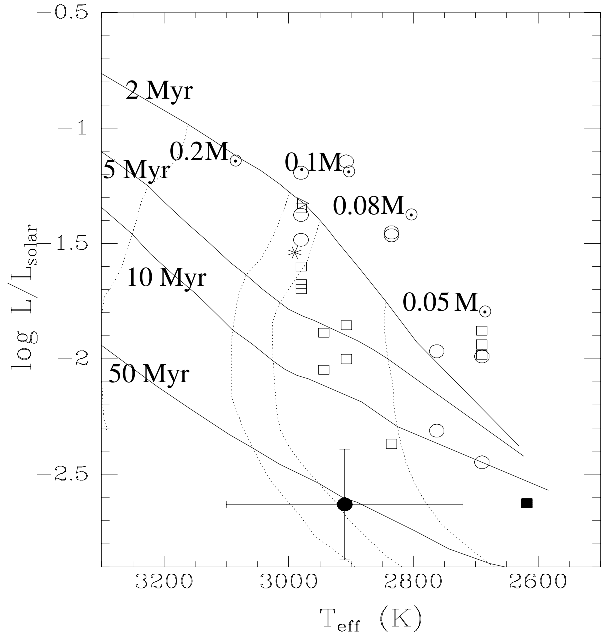

Fig. 7. Position of LS-RCrA 1 (filled circle) and LS-RCrA 2 (asterisk) in a temperature-luminosity diagram, compared with the results of theoretical evolutionary models for low mass stars and brown dwarfs (Baraffe et al. 1998). The same objects that appear in Fig. 5 are plotted here, showing the distinct location of LS-RCrA 1 with respect to other young objects studied so far. Symbols have the same meanings as in Fig. 5. The error bar in temperature has a length given by the difference between the Luhman 1999 temperature scale for young objects and that of Leggett et al. 1996 for field M dwarfs. The length of error bar in luminosity corresponds to the additive effects of a variation of 0.13 mag in extinction, 0.25 mag in the distance modulus, and 0.20 mag in bolometric correction, with the signs that produce a maximum deviation in $\log L$, as explained in the text. Error bars due to photometric and spectral classification uncertainties are small in comparison to these calibration-dependent effects. It is important to note that calibration-dependent errors in the temperature scale and in the bolometric correction would shift all the objects in this figure, and not only LS-RCrA 1.

to its actual value, this is, that we have underestimated the extinction and the distance, and overestimated the bolometric correction. Varying the values of those quantities by +0.13, +0.25, and -0.20 mag as discussed above, we still obtain $\log L(\mathrm{L}_\odot) = -2.39$, which barely brings the luminosity to the level of that of the faintest brown dwarf known in Chamaeleon I -despite of the fact that LS-RCrA 1 is 1-2 spectral subclasses earlier.

3.5. Comparison to low-mass evolutionary models

A more detailed comparison with the predictions of existing pre-main sequence evolutionary models is useful in providing an appreciation of the difficulties encountered when trying to use the spectral and photometric properties of LS-RCrA 1 to derive its intrinsic properties, as is usually done in the study of the low-mass component of star forming regions. This discussion is based on the pre-main sequence tracks of Baraffe et al. 1998, but virtually unchanged results are encountered when using other recent tracks such as those of Burrows et al. 1997 and D'Antona & Mazzitelli 1997.

Figure 7 shows the position of LS-RCrA 1 on the temperature-luminosity diagram as compared to pre-main sequence tracks and isochrones. Also shown are the same late-type objects from other star forming regions plotted in Fig. 5, for which both spectral classifications in the visible and JHK photometry are available. To ensure the homogeneity of the comparison, we have estimated luminosities and temperatures for all these objects in the same way as described above, rather than using published estimates of these quantities based on different methods. In this respect, it is important to note that the error bars plotted at the position of LS-RCrA 1 in Fig. 7 are mostly due to uncertainties in the translation of observed to intrinsic properties, which dominate over the uncertainties associated with the photometry or the spectral type determination alone. Therefore, shifting the position of LS-RCrA 1 along its error bars to account for systematic errors in the calibrations (except for the distance and the extinction) would also imply similar shifts of the other objects in the same direction, leaving the relative differences among them almost unchanged. In other words, the large error bars associated with the intrinsic properties of LS-RCrA 1 do not affect the conclusion that such properties are markedly different from those of other late-type young objects discovered so far.

While a comparison with theoretical model predictions shows that the positions of very young late M-type objects agree well in general with the expected ages of star forming regions, this is not the case for LS-RCrA 1 if the age implied by this comparison is taken at face value. The inferred 50 Myr of age for LS-RCrA 1 is over one order of magnitude older than the age assigned by Wilking et al. 1997 to the R CrA complex. Neuhäuser et al. 2000 also find ages in the $\sim 1 - 10$ Myr interval for more massive, X-ray emitting members of this region. The large discrepancy between the inferred age of LS-RCrA 1 and that of the R CrA complex in particular, or of star forming regions in general, lead us to look for alternative explanations to its observed properties.

Let us recall in this respect that a distinctive property of LS-RCrA 1 not shared by any other of the objects plotted in Fig. 7 is the very strong emission lines indicating intense accretion on the central object. Pre-main sequence evolutionary models do not take accretion into account, thus neglecting the effects that it may have on the temperature and luminosity of the object. This is justified by the relatively small accretion rates usually derived, but such an assumption may not apply to LS-RCrA 1. Therefore, the possibility that the photospheric temperature and luminosity are substantially affected by the present accretion and that published zero-accretion pre-main sequence tracks may not be useful for the present case should not be ruled out.

Although there are no available calculations of how strong accretion on a very low mass object modify its position in the $(T_{\rm eff}, \log L)$ diagram, the effect has been considered for moderate accretion rates and higher masses by Hartmann et al. 1997 and Siess et al. 1997 and gives a hint on the directions in which those modifications may go. The results of both studies indicate that accretion increases both the surface temperature and the luminosity of the central object with respect to the values that it would have with the same age and mass in the absence of accretion. The net direction of the shift in the $(T_{\rm eff}, \log L)$ diagram moves the object to the position that a more massive non-accreting object with a slightly older age would have. Evolutionary models of accreting pre-main-sequence stars focus on the effect of accretion in the interior structure of the object, and particularly on the consequences of extended deuterium burning at the core due to the continued replenishment of the deuterium supply thanks to freshly accreted gas. One of these consequences is an increase of the effective temperature, that is attained with a radius (and therefore a luminosity) smaller than that of a non-accreting object of the same age and temperature, which in turn would have a higher mass; hence the direction of the shift in the $(T_{\rm eff}, \log L)$ diagram. These models do not take into account the effects of accretion on the atmosphere's chemistry and structure, which is an essential boundary condition determining the evolution of very low mass objects (Chabrier and Baraffe 2000). However, assuming that the qualitative effects of accretion are the same on LS-RCrA 1, we thus infer that its age is actually younger than its position in the $(T_{\rm eff}, \log L)$ suggests, in agreement with the expectation from its membership in the R CrA star forming region. Moreover, if this interpretation is correct then its mass should be considerably less than the $\simeq 0.08$ M$_\odot$ derived from Fig. 7. Assuming that the true age is 10 Myr and that the luminosity is unaffected by accretion, models assign a mass $M \simeq 0.02$ M$_\odot$. This is still a conservative assumption, as the mean age in R CrA is even younger and accretion, at least at higher masses, leads to an increase of the luminosity. Thus, it is possible that LS-RCrA 1 is actually a young low-mass brown dwarf, rather than a relatively old transition object. We should caution however that this interpretation is a rather speculative one, based on a large extrapolation of Hartmann et al. and Siess et al.'s results in both mass and accretion rate.

An alternative explanation may be that the light of LS-RCrA 1 actually comes from a flaring circumstellar disk seen nearly edge-on, whose external layers are illuminated by the central object and reprocess its emitted energy by absorption and scattering. Adaptive optics observations have allowed in recent years to spatially resolve such disks around some objects in nearby star forming regions such as Orion, Taurus, and ρ Ophiuchi (Burrows et al. 1996, McCaughrean & O'Dell 1996, Monin & Bouvier 2000, Stapelfeldt et al. 1998, Brandner et al. 2000), showing that the visible and near infrared images are actually due to scattered light from a central object too embedded to be directly detected. Fitting scattering models (Lazareff et al. 1990, Burrows et al. 1996) to the observed spatial morphology and the spectral energy distribution leads to the derivation of the structural parameters of the circumstellar disks and the scattering properties of the dust. In this geometry the observed light, which is the stellar light reflected and scattered on the disk surface, suffers little circumstellar extinction and, besides an obvious dimming of the light of the central object, there is little effect on the colors of the emergent spectral energy distribution as compared to the intrinsic colors of the central object. This is seen for example in HH 30 (Burrows et al. 1996) and HV Tau C (Woitas & Leinert 1998, Monin & Bouvier 2000), two objects for which circumstellar disks have been resolved but whose visible and near-infrared colors do not indicate at first sight the existence of a heavily embedded object (the situation may be different for the objects reported by Brandner et al. 2000 in ρ Ophiuchi, although in those cases the very red colors are probably due to foreground extinction). HV Tau C is particularly interesting in this respect: the colors reported by Woitas & Leinert 1998 between the V and K bands are remarkably similar to those of LS RCrA 1, while the central object is of an earlier type as deduced from the absence of visible molecular absorption bands in the underlying spectrum. It also displays strong emission lines, including forbidden lines with equivalent widths similar to those that we observe in LS RCrA 1, although H$_\alpha$ has a far lower intensity relative to them (Monin & Bouvier 2000). If the low apparent brightness of LS-RCrA 1 is due to blocking by a nearly edge-on circumstellar disk, and assuming that its intrinsic luminosity is the normal one for a 3 Myr old M6.5 object, the net effect of the disk (extinction plus scattering) is equivalent to an approximately grey extinction of ~ 2.5 mag, less than for HV Tau C where it may be estimated to be $\sim 4-5$ mag (much of the uncertainty comes from the observed variability of the source; Monin & Bouvier 2000). An even larger equivalent extinction is derived for HH 30 (Burrows et al. 1996), suggesting that the plane of the hypothetical disk of LS-RCrA 1 may be less aligned with the line of sight than in those other two cases. The characteristic sizes of the scattering-dominated emission regions in spatially resolved edge-on disks is measured to be of order $\sim$ 100 AU, needing angular resolutions of few tenths of arcseconds in order to resolve them in nearby star forming regions, including R Coronae Australis. Our best-quality images, those obtained with ISAAC in the K band in April 2001, have a full-width at half maximum of $0''38$, or 60 AU at the adopted distance of R Coronae Australis, and LS-RCrA 1 appears unresolved in them. This is already a fairly constraining scale for any possible structure around LS-RCrA 1, which could be easily improved using adaptive optics imaging.

4. Discussion

The combination of late spectral type, strong emission lines, class I-like features together with absence of near infrared excess, and unusually old age inferred from comparison with evolutionary models all contribute to make LS-RCrA 1 a unique object. It seems clear from the tentative explanations given to some of these features that accretion, and perhaps geometry, play a very important role in determining the observational properties of this object, and it may be of interest at this point to note the existence of two other known very late-type objects that have been mentioned in previous Sections and that may be useful for comparative studies. The first one is Oph162349.8-242601, a M8.5 brown dwarf in ρ Ophiuchi whose precise spectral classification was established by Luhman et al. 1997. Despite its later spectral type, the photometric properties of that object are very similar to those of LS-RCrA 1, and it also shows strong H_α emission although at only 20% of the level that we detect for the latter. Although Oph162349.8-242601 does not display signs of near-infrared excess either (it occupies virtually the same position as LS-RCrA 1 in Fig. 5), the existence of a considerable *reservoir* of circumstellar material around it is inferred from its detection in deep ISOCAM images at 4.5 μm (Comerón et al. 1998). Unfortunately, no published observations longwards of 2.2 μm exist of LS-RCrA 1: despite its position near the center of the R CrA complex, it lies close to a region of strong mid-infrared emission that had to be avoided in the ISOCAM survey of Olofsson et al. 1998 for detector saturation reasons. The mid-infrared excess is also displayed by the other similar object that we wish to refer to, GY 11, also in ρ Ophiuchi. No visible-red spectroscopy is available as yet for this deeply embedded object, but normal K-band late-type spectroscopic features have been observed by Williams et al. 1995 and Wilking et al. 1999. Interestingly, as noted before, this object also shows H_2 emission. It thus seems that the conclusion of Greene & Lada 1996a, who noted that this line is almost exclusively observed in the spectra of class I objects having no CO absorption bands and only very rarely in class II sources, may not apply for objects of very low mass and temperature such as GY 11 and LS-RCrA 1. A possible explanation for this may reside in the absence of dust at sufficiently high temperatures to produce any significant veiling of the near-infrared photospheric lines in such cool objects.

Follow-up observations of LS-RCrA 1 are clearly very desirable to serve several purposes. In the first place, high resolution imaging of LS-RCrA 1 is needed to look for direct evidence of a possible edge-on circumstellar disk. Its detection would explain the anomalously low luminosity of LS-RCrA 1 given its assumed age and its spectral type, while the non-detection of any traces of small-scale resolved emission at the position of LS-RCrA 1 would instead lend support to an accretion-based origin for the low luminosity. On the monitoring side, and as indicated at the beginning of Section 3, photometry both in the visible and the infrared indicate that the object is variable with an amplitude of at least a few tenths of a magnitude. T Tauri-like variability in young objects can have different causes (Herbst et al. 1994), and regular photometric observations are of great use in the modeling of surface features such as cool spots or the hot spots appearing at the base of the accretion column in the photosphere. Multiband photometric measurements are for instance able to constrain the temperature, rotation period, and extent of a hot spot, as described by Fernández & Eiroa 1996. Photometric monitoring would thus be very useful in further constraining the accretion properties of LS-RCrA 1, enlarging the data recently obtained for very cool objects (Bailer-Jones & Mundt 2001) with a highly singular one.

Spectroscopic monitoring would also be very useful to explore variability of the accretion and mass loss diagnostic lines, as well as of the underlying continuum. The unique combination of intense accretion and mass loss on one side, and low mass, temperature and luminosity on the other, make LS-RCrA 1 an important testbench for models of stellar-circumstellar interaction. In particular, high resolution observations of H_α and other lines would be of the highest interest to check for accretion-related signatures that are sensitive to the details of the process and of the region where line formation takes place (e.g. Calvet & Gullbring 1998, Muzerolle et al. 2001). They would also allow detailed modeling leading to quantitative estimates of the mass accretion and loss rates.

5. Conclusions

We have presented visible and near-infrared imaging and spectroscopy of a faint late-type object in the R Coronae Australis star forming region, LS-RCrA 1, displaying a spectrum with very strong emission lines similar to that of classical T Tauri stars. Our conclusions after studying both the emission line spectrum and the underlying continuum may be summarized as follows:

- The underlying spectrum is typical of that of a M6.5 ($\pm$0.5) very young stellar object. Although veiling is likely to be present given the intensity of the emission lines that indicate accretion, the present spectral classification should be little affected by it.
- The lines in the rich emission-line spectrum, which includes numerous forbidden lines, have unprecedented intensities for an object of such a late spectral type, with an equivalent width $W(H_\alpha) = 360$ Å. The line ratios cannot be explained by mass accretion or outflow only; instead, both processes must be operating simultaneously.
- BVR_CI_CJHK colors are typical for a late M object with almost no obscuration. The photometry at two different epochs shows signs of variability. Follow-up photometric monitoring would be very helpful in establishing and modeling its detailed causes.
- The photometric properties in the near-infrared (JHK) band are the same as those of late-type dwarfs objects without excess due to circumstellar material. However, the K-band spectrum is not typical of a late-type object: the CO bands starting at 2.29 μm are much less deep and atomic lines are not visible down to a $W = 3$ Å level. At the same time, H_2 emission typical of

outflows, usually seen only in objects with steeply rising K-band spectral energy distributions, is detected also in LS-RCrA 1. We suggest that the almost featureless spectrum in such an object lacking K-band excess emission may be due to line filling by emission in the funnel-flow of accretting matter from a magnetically disrupted cool circumstellar disk, rather than continuum veiling by dust as is commonly interpreted in other cases.

- The very low luminosity ($\log L = -2.63$) that we derive for LS-RCrA 1 makes it far less luminous than any other object of similar spectral type in star forming regions, and would imply an age above $\sim$ 50 Myr when the position in the temperature-luminosity diagram is compared to results of pre-main sequence evolutionary models. This age is over one order of magnitude older than that derived from the rest of the population of the R Coronae Australis star forming region, and hints to a different reason for the unusual observational properties of LS-RCrA 1. We speculate that the early evolution of LS-RCrA 1 may be substantially modified by intense accretion, to the point of invalidating the comparison with zero-accretion evolutionary models. A qualitative extrapolation of the results of models of T Tauri stars with accretion suggests that LS-RCrA 1 may actually have a mass well below the substellar limit, perhaps being an intensely accreting low mass brown dwarf. We also consider as a possible alternative explanation the presence of a nearly edge-on circumstellar disk, which reflects and scatters the stellar photospheric light. In such a geometry, one expects to observe nearly the intrinsic colours of the unobscured object, with a small additional component due to scattered light, which makes the object appears bluer at short wavelengths. This is actually the case for LS-RCrA 1, its (B-V) colour being slightly too blue for an M6 spectral type. In this latter case, observations with high angular resolution ($\sim 0''1$ or better) may be expected to allow direct, spatially resolved imaging of the disk, which so far has not been detected down to a linear resolution of 60 AU.

LS-RCrA 1 is the latest-type object for which signposts of strong accretion and mass loss have been detected so far, implying that both of these processes are linked and can take place with great intensity even beyond the bottom of the stellar mass sequence. The available observational material suffices to hint at interesting differences with their well studied high mass counterparts. On the other hand, the similarities in some aspects between LS-RCrA 1 and brown dwarfs such as Oph162349.8-242601 and GY 11, that also display signs of important amounts of circumstellar matter, stresses the need to extend existing detailed models of accretting young stars towards much lower masses than those assumed so far. These models, as well as future and more detailed observations of LS-RCrA 1 and similar objects, are needed to complete our understanding of accretion and star formation over the complete range of stellar and substellar masses.

Acknowledgements. We are very pleased to thank the staffs of both La Silla and Paranal Observatories for excellent support during our observations, especially to Drs. Alessandro Pizzella and Chris Lidman, and to Mr. Fernando Selman. Dr. Wolfgang Brandner is especially thanked for pointing out to us the possibility that the low apparent luminosity of the object described here may be due to an edge-on circumstellar disk. We also thank the ESO User Support Group for assistance with the preparation of the FORS2 Service Mode observations, and the astronomers in charge of service observing at Kueyen (VLT UT2) when our FORS2 observations were carried out. We acknowledge the ESO Director's Discretionary Time Committee and the Observing Panel Commitee for the allocation of observing time at different ESO telescopes. We appreciate very much the comments and suggestions done by the referee, J. Bouvier. MF was partially supported by the Spanish grant PB97-1438-C02-02.

References

Appenzeller, I., & Mundt, R., 1989, A&A Rev., 1, 291.
Bailer-Jones, C.A.L., & Mundt, R., 2001, A&A, 367, 218
Bally, J., & Devine, D. 1994, ApJ 428, L65.
Baraffe, I., Chabrier, G., Allard, F., & Hauschildt, P.H., 1998, A&A, 337, 403.
Barsony, M., Kenyon, S.J., Lada, E.A., & Teuben, P.J., 1997, ApJS, 112, 109.
Bertout, C. 1989, ARA&A, 27, 351.
Bessell, M.S., & Brett, J.M., 1988, PASP, 100, 1134.
Böhm, K.-H., & Goodson, A.P. 1997, in "Herbig-Haro flows and the birth of stars", eds. B. Reipurth & C. Bertout, Kluwer Acad. Publ.
Brandner, W., Sheppard, S., Zinnecker, H., Close, L., Iwamuro, F., Krabbe, A., Maihara, T., Motohara, K., Padgett, D.L., & Tokunaga, A., 2000, A&A, 364, L13.
Burrows, C.J., Stapelfeldt, K.R., Watson, A.M., Krist, J.E., Ballester, G.E., Clarke, J.T., Crisp, D., Gallagher, J.S., Griffiths, R.E., Hester, J.J., Hoessel, J.G., Holtzmann, J.A., Mould, J.R., Scowen, P.A., Trauger, J.T., & Westphal, J.A., 1996, ApJ, 473, 437.
Burrows, A., Marley, M., Hubbard, W.B., Lunine, J.I., Guillot, T., Saumon, D., Freedman, R., Sudarsky, D., & Sharp, C., 1997, ApJ, 491, 856.
Cabrit, S., Edwards, S., Strom, S.E., & Strom, K.M., 1990, ApJ, 354, 687.
Casali, M.M., & Matthews, H.E., 1992, MNRAS, 258, 399
Casali, M.M., & Eiroa, C., 1996, A&A, 306, 427
Calvet, N., & Gullbring, E., 1998, ApJ, 509, 802.
Chabrier, G., & Baraffe, I., 2000, ARA&A, 38, 337
Comerón, F., Rieke, G.H., Claes, P., Torra, J., & Laureijs, R.J., 1998, A&A, 335, 522.
Comerón, F., Rieke, G.H., & Neuhäuser, R., 1999, A&A, 343, 477.
Comerón, F., Neuhäuser, R., & Kaas, A.A., 2000, A&A 359, 269.
D'Antona, F., & Mazzitelli, I., 1997, Mem. S.A.It., 68, 807.
Dougados, C., Cabrit, S., Lavalley, C., & Ménard, F., 2000, A&A, 357, L61
Fernández, M., & Eiroa, C. 1996, A&A 310, 143.
Fluks, M.A., 1998, PhD Thesis, Univ. of Amsterdam.
Graham, J.A., 1993, PASP, 105, 561.
Graham, J.A., & Heyer, M.H., 1988, PASP, 100, 1529.
Greene, T.P., & Lada, C.J., 1996a, AJ, 112, 2184.

Greene, T.P., & Lada, C.J., 1996b, ApJ, 461, 345.
Gullbring, E., Hartmann, L., Briceño, C., & Calvet, N., 1998, ApJ, 492, 323.
Gullbring, E., Calvet, N., Muzerolle, J., & Hartmann, L., 2000, ApJ, 544, 927.
Hamann, F., 1994, ApJS, 93, 485.
Hamuy, M., Walker, A.R., Suntzeff, N.B., Gigoux, P., Heathcote, S.R., & Phillips, M.M., 1992, PASP, 104, 533.
Hartmann, L., 1998, "Accretion processes in star formation" Cambridge Univ. Press.
Hartmann, L., Cassen, P., & Kenyon, S.J., 1997, ApJ, 475, 770.
Heathcote, S., Reipurth, B., & Raga, A.C., 1998, AJ 116, 1940.
Herbig, G.H., & Bell, K.R. 1988, Lick Obs. Bull. No.1111, p.1
Herbst, W., Herbst, D.K., Grossman, E.J., & Weinstein, D., 1994, AJ, 108, 1906.
Kenyon, S.J., & Hartmann, L., 1995, ApJS, 101, 117.
Kirkpatrick, J.D., Henry, T.J., & McCarthy, D.W., 1991, ApJS, 77, 417.
Kleinmann, S.G., & Hall, D.N.B., 1986, ApJS 62, 501
Knude, J., & Høg, E., 1999, A&A, 341, 451.
Krautter, J., 1986, A&A, 161, 195.
Krautter, J., Reipurth, B., & Eichendorf, W. 1984, A&A, 133, 169.
Lada, C.J., & Adams, F.C., 1992, ApJ, 393, 278.
Lawson, W.A., Feigelson, E.D., & Huenemoerder, D.P., 1996, MNRAS, 280, 1071.
Lazareff, B., Pudritz, R.E., & Monin, J.-L., 1990, ApJ, 358, 170.
Leggett, S.K., Allard, F., Berriman, G., Dahn, C.C., & Hauschildt, P.H., 1996, ApJS, 104, 117.
Luhman, K.L., 1999, ApJ, 525, 466.
Luhman, K.L., 2000, ApJ, 544, 1044.
Luhman, K.L., & Rieke, G.H., 1998, ApJ, 497, 354.
Luhman, K.L., Liebert, J., & Rieke, G.H., 1997, ApJ, 489, L165.
Marraco, H.G., & Rydgren, A.E., 1981, AJ, 86, 62.
Martin, S.C., 1996, ApJ, 470, 537.
Martin, S.C., 1997, ApJ, 478, L33.
McCaughrean, M.J., & O'Dell, C.R., 1996, AJ, 111, 1977.
Monin, J.-L., & Bouvier, J., 2000, A&A, 356, L75.
Muzerolle, J., Briceño, C., Calvet, N., Hartmann, L., Hillenbrand, L., & Gullbring, E., 2000, ApJ, 545, L141.
Muzerolle, J., Calvet, N., & Hartmann, L., 2001, ApJ, 550, 944
Neuhäuser, R., Walter, F.M., Covino, E., Alcalá, J.M., Wolk, S.J., Frink, S., Guillout, P., Sterzik, M.F., & Comerón, F., 2000, A&AS, 146, 323.
Oliva, E., & Origlia, L., 1992, A&A, 254, 466.
Olofsson, G., Huldtgren, M., Kaas, A.A., Bontemps, S., Nordh, L., Abergel, A., André, P., Boulanger, F., Burgdorf, M., Casali, M.M., Cesarsky, C.J., Davies, J., Falgarone, E., Montmerle, T., Perault, M., Persi, P., Prusti, T., Puget, J.L., & Sibille, F., 1998, A&A, 350, 883.
Patten, B.M., 1998, ASP Conf. Ser. 154, 1755.
Reipurth, B., Bally, J., Graham, J.A., Lane, A.P., & Zealey, W.J. 1986, A&A 164, 51
Rieke, G.H., & Lebofsky, M.J., 1985, ApJ, 288, 618.
Schwartz, R.D., 1977, ApJS, 35, 161.
Siess, L., Forestini, M., & Bertout, C., 1997, A&A, 326, 1001
Shull, J.M., & Beckwith, S.V.W., 1982, ARA&A 20, 163
Stapelfeldt, K.R., Krist, J.E., Ménard, F., Bouvier, J., Padgett, D.L., & Burrows, C.J., 1998, ApJ, 502, L65.
Wilking, B.A., McCaughrean, M.J., Burton, M.G., Giblin, T., Rayner, J.T., & Zinnecker, H., 1997, AJ, 114, 2029.
Wilking, B.A., Greene, T.P., & Meyer, M.R., 1999, AJ, 117, 469.
Williams, D.M., Comerón, F., Rieke, G.H., & Rieke, M.J., 1995, ApJ, 454, 144.
Woitas, J., & Leinert, Ch., 1998, A&A, 338, 122
Zapatero Osorio, M.R., Martín, E.L., & Rebolo, R., 1997, A&A, 323, 105.
Zapatero Osorio, M.R., Béjar, V.J.S., Martín, E.L., Rebolo, R., Barrado y Navascués, D., Bailer-Jones, C.A.L., & Mundt, R., 2000, Science, 290, 103.
de Zeeuw, P.T., Hoogerwerf, R., de Bruijne, J.H.J., Brown, A.G.A., & Blaauw, A., 1999, AJ, 117, 354.